Hall plateau diagram for the Hofstadter butterfly energy spectrum

Mikito Koshino and Tsuneya Ando
Department of Physics, Tokyo Institute of Technology, 2-12-1 Ookayama, Meguro-ku, Tokyo 152-8551, Japan
(Received 31 October 2005; revised manuscript received 10 February 2006; published 5 April 2006)

We extensively study the localization and the quantum Hall effect in the Hofstadter butterfly, which emerges in a two-dimensional electron system with a weak two-dimensional periodic potential. We numerically calculate the Hall conductivity and the localization length for finite systems with the disorder in general magnetic fields, and estimate the energies of the extended levels in an infinite system. We obtain the Hall plateau diagram on the whole region of the Hofstadter butterfly, and propose a theory for the evolution of the plateau structure with increasing disorder. There we show that a subband with the Hall conductivity ne^2/h has $|n|$ separated bunches of extended levels, at least for an integer $n \leqslant 2$. We also find that the clusters of the subbands with identical Hall conductivity, which repeatedly appear in the Hofstadter butterfly, have a similar localization property.

DOI: 10.1103/PhysRevB.73.155304 PACS number(s): 73.43.−f, 73.50.−h, 71.30.+h

I. INTRODUCTION

A two-dimensional (2D) electron system with a 2D periodic potential is expected to exhibit an intricate energy spectrum in a strong magnetic field, which is called the Hofstadter butterfly. When the magnetic length is of the order of the lattice constant, the interplay of the Landau quantization and Bragg reflection yields a fractal-like series of energy gaps, which depends sensitively on the number of magnetic flux quanta per unit cell,[1]

$$\phi = \frac{Ba^2}{h/e},$$

where B is the amplitude of the constant magnetic field and a is the lattice constant. Moreover, it is shown that each subband carries a quantized Hall conductivity, which varies with the energy gaps in a nontrivial manner.[2] The recent developments in experimental techniques make it possible to fabricate a two-dimensional superlattice on a 2D electron gas (2DEG). Evidence of the fractal energy spectrum was found in a superlattice patterned on $GaAs/Al_xGa_{1-x}As$ heterostructures,[3,4] where the Hall conductivity changes nonmonotonically as the Fermi energy transfers from one gap to another.

From the theoretical side, it is intriguing to consider the magnetotransport in this intricate energy spectrum. Broadening of the density of states[5,6] and the conductivity[5] were investigated for the Hofstadter butterfly within the self-consistent Born approximation. For the localization regime, we expect that, by analogy with unmodulated 2D systems, the extended levels appear only at certain energies in the Hofstadter spectrum, and $\sigma_{xy}(E)$ will turn into a series of Hall plateaus separated by those energies.

The evolution of the extended states as a function of the disorder was proposed for several flux states in the Hofstadter butterfly.[7–9] A finite-size scaling analysis was performed for a 2D system modulated by a weak periodic potential and it was found that the modulation does not change the critical exponent at the center of the Landau level.[10,11] Previously we have numerically calculated the Hall conductivity in weakly modulated 2D systems at several fluxes and studied the effect of the localization on the quantum Hall effect in the Hofstadter butterfly.[12] There we determined the energies of the extended levels from the scaling behavior of the Hall conductivity in finite systems.

In this paper, following the line of the previous work, we present an extensive study of the quantum Hall effect in a single Landau level in the presence of the two-dimensional periodic potential. We numerically calculate the Hall conductivity and the localization length in general magnetic fluxes, using the exact diagonalization of the Hamiltonian for finite systems. We determine the energies of the extended levels in an infinite system by analyzing the size dependence in the Hall conductivity, and find that those energies always coincide with the points where $\sigma_{xy}/(-e^2/h)$ becomes $n+1/2$ (n is an integer) in finite systems. In particular, we resolved *two* separated extended levels in a subband carrying the Hall conductivity by $2e^2/h$. We propose a possible scenario for the evolution of the extended levels with increasing disorder for several fluxes, which suggests that the Hall plateau structure changes through the pair annihilation and/or pair creation of the extended levels. We survey the Hall conductivity over the whole region of the Hofstadter butterfly, to find that electronic structure with similar Hall conductivity and localization length appears in a self-similar manner at different fluxes, reflecting the fractal property of the ideal spectrum.

II. FORMULATION

We first prepare the formulation to describe a Bloch electron in magnetic fields. Let us consider a two-dimensional system in a uniform magnetic field with a periodic potential V_p and a disorder potential V_d,

$$H = \frac{1}{2m}(\boldsymbol{p} + e\boldsymbol{A})^2 + V_p + V_d. \tag{1}$$

We assume that V_p has a square form,

$$V_p = V\cos\frac{2\pi}{a}x + V\cos\frac{2\pi}{a}y,$$

and the disorder potential is composed of randomly distributed δ potentials $\pm v_0$ with the number per unit area n_i, where the amounts of the positive and negative scatterers are taken to be equal. We consider only the lowest Landau level ($N=0$), assuming that the magnetic field is strong enough and the mixing of the Landau levels is neglected. In the Landau gauge, the basis can be taken as

$$|0,k_y\rangle = \sqrt{\frac{1}{\sqrt{\pi}lL_y}}\exp(ik_y y)\exp\left(-\frac{(x+k_y l^2)^2}{2l^2}\right) \quad (2)$$

with the magnetic length $l=\sqrt{\hbar/eB}$. The matrix elements of V_p are then written

$$\langle 0,k_y'|V_p|0,k_y\rangle = \delta_{k_y',k_y}2Ve^{-\pi/2\phi}\cos\frac{k_y a}{\phi} + (\delta_{k_y',k_y+2\pi/a}+\delta_{k_y',k_y-2\pi/a})Ve^{-\pi/2\phi}. \quad (3)$$

In an ideal system ($V_d=0$), the wave function can then be expanded as

$$\psi_{k_y}(\boldsymbol{r}) = \sum_m c_m(k_y)\left|0,k_y-\frac{2\pi}{a}m\right\rangle, \quad (4)$$

with Bloch wave number k_y ranging from $-\pi/a$ to π/a. The Schrödinger equation is then reduced to Harper's equation,

$$Ve^{-\pi/2\phi}(c_{m+1}+c_{m-1}) + 2Ve^{-\pi/2\phi}\cos\left(\frac{k_y a-2\pi m}{\phi}\right)c_m = Ec_m. \quad (5)$$

In a rational flux $\phi=p/q$ (p,q are coprime integers), the equation becomes periodic in m with a period p, which corresponds to a distance qa in the center coordinate along the x axis, so that we have the Bloch condition $c_{m+p}=e^{ik_x qa}c_m$ with another Bloch wave number k_x from $-\pi/(qa)$ to $\pi/(qa)$. As a result, we have p independent states for each of $\boldsymbol{k}=(k_x,k_y)$ in the Landau level, so that we can label the wave function as ψ_{nk} on a q-folded Brillouin zone with the subband index $n=1,2,\ldots,p$. We can decompose the wave function as $\psi_{nk}(\boldsymbol{r})=e^{i(k_x x+k_y y)}u_{nk}(\boldsymbol{r})$, where u satisfies the magnetic Bloch condition

$$u(x,y+b)=u(x,y),$$

$$u(x+qa,y)=e^{2\pi ipy/a}u(x,y). \quad (6)$$

Figure 1 shows the energy spectrum in the lowest Landau level at $V_d=0$ plotted against ϕ. The intricate band structure is due to the number of subbands p, which is not a continuous function of ϕ. We can show that p subbands never overlap so that we always have $p-1$ energy gaps inside the Landau level. The total width of the spectrum scales with the factor $e^{-\pi/2\phi}$ in Eq. (5), and shrinks as the flux becomes smaller. The lower panel shows the zoom out of the spectrum covering from $\phi=0$ to 10. We can see that, on going to a higher field, a series of subbands splits away from the center toward higher and lower energies. These are identified in the semiclassical picture as the quantization of the electron motion along the equipotential line around the bottom or the top of the periodic potential. The widths of those levels become narrower for larger ϕ because the coupling between different potential valleys becomes exponentially small as the magnetic length becomes smaller.

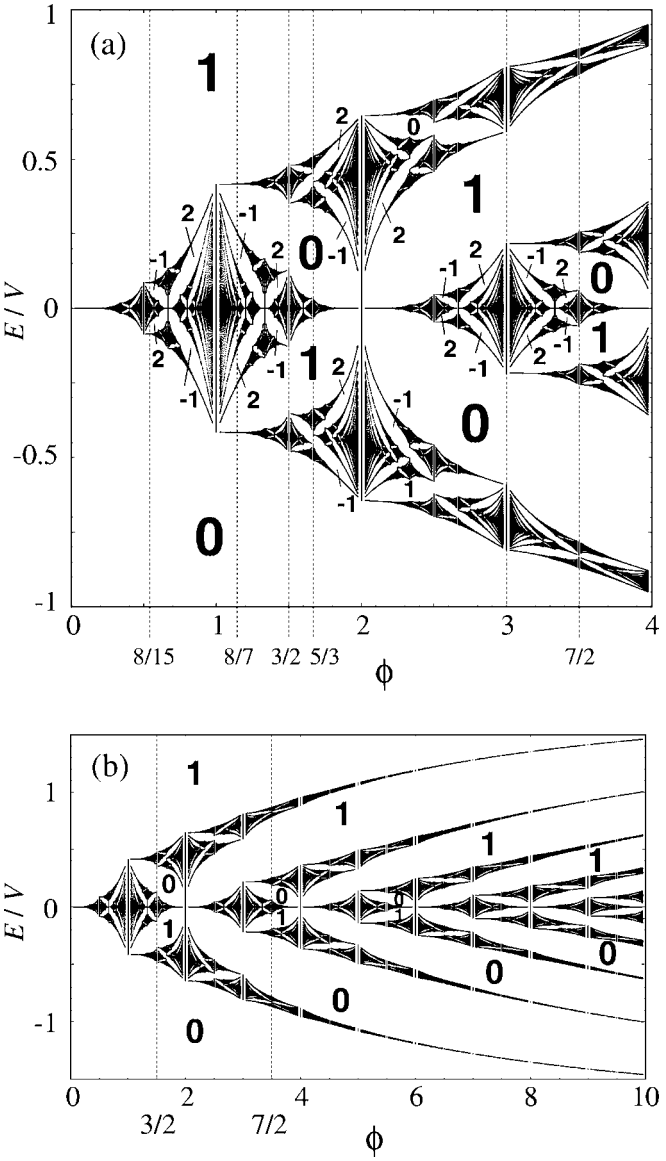

FIG. 1. (a) Ideal energy spectrum of the lowest Landau level in a weakly modulated two-dimensional system, plotted against the magnetic flux ϕ. Integers inside gaps indicate the quantized Hall conductivity in units of $(-e^2/h)$. (b) Zoom out of (a).

The Hall conductivity σ_{xy} is calculated by the Kubo formula as

$$\sigma_{xy} = \sum_{\epsilon_\alpha<E_F}\sum_{\epsilon_\beta\neq\epsilon_\alpha}\frac{\langle\alpha|v_x|\beta\rangle\langle\beta|v_y|\alpha\rangle-\langle\alpha|v_y|\beta\rangle\langle\beta|v_x|\alpha\rangle}{(\epsilon_\alpha-\epsilon_\beta)^2}, \quad (7)$$

where E_F is the Fermi energy and ϵ_α the energy of the eigenstate $|\alpha\rangle$ in the lowest Landau level. This is rewritten in an ideal system as[2]

$$\sigma_{xy} = \frac{e^2}{2\pi h} \sum_n \int_{E<E_F} d^2k \, 2 \, \mathrm{Im} \left(\left\langle \frac{\partial u_{nk}}{\partial k_x} \middle| \frac{\partial u_{nk}}{\partial k_y} \right\rangle \right), \quad (8)$$

where the summation is taken over all the occupied states. It is shown that the contribution from all the states in *one* subband is always quantized in units of $-e^2/h$.[2] So we have an integer Hall conductivity when the Fermi energy E_F is in every gap, since it simply becomes the summation of the integers for all the subbands below E_F. In such a gapped situation, we have a useful expression for the Hall conductivity called the Středa formula,[13] which is directly derived from the Kubo formula (7). This is written as

$$\sigma_{xy} = -e \frac{\partial n}{\partial B}, \quad (9)$$

where n is the number of states below the Fermi energy per unit area and B is the magnetic field. In Fig. 1, we put the value of the Hall conductivity for each of the gaps obtained by this formula. The contribution by one subband, $\Delta\sigma_{xy}$, is obtained as the difference in σ_{xy} between the gaps above and below the subband. In Fig. 1(b), the series of branches mentioned above always carries $\Delta\sigma_{xy}=0$, since those subbands, coming from the localized orbitals around the potential minima or maxima, contain a constant number of states $n=1/a^2$ which is independent of the magnetic field.

III. LOCALIZATION AND THE QUANTUM HALL EFFECT

We now move on to the disordered system to investigate the localization and the quantum Hall effect. Here we numerically diagonalize the Hamiltonian (1) of finite systems of $L\times L$ with $L=Ma$ (M is an integer), and calculate the localization length L_{loc} and the Hall conductivity σ_{xy} as functions of Fermi energy. The localization length is obtained from the system size dependence of the Thouless number $g(L)$, by assuming that $g(L)$ behaves as $\exp(-L/L_{\mathrm{loc}})$, where $g(L)$ is defined as the ratio of the difference in the eigenenergies between periodic and antiperiodic boundary conditions to the mean level spacing ΔE. The Hall conductivity is calculated by the Kubo formula (7) with the exact eigenstates in the disordered system, where the mixing between different Landau levels is taken into account within the lowest order in $(V_p+V_d)/(\hbar\omega_c)$ with $\omega_c=eB/m$ being the cyclotron frequency. Every quantity is averaged over a number of different samples.

In the strong disorder regime, the energy scale of the disorder is characterized by

$$\Gamma = \sqrt{\frac{4n_i v_0^2}{2\pi l^2}},$$

which represents the increasing width of the Landau level in absence of the periodic potential.[14] This parameter is relevant as long as the disorder is strong enough to destroy the band structure inside the Landau level. In the weak disorder limit, on the other hand, the relevant parameter is the increasing width of the Bloch subband, which is written as

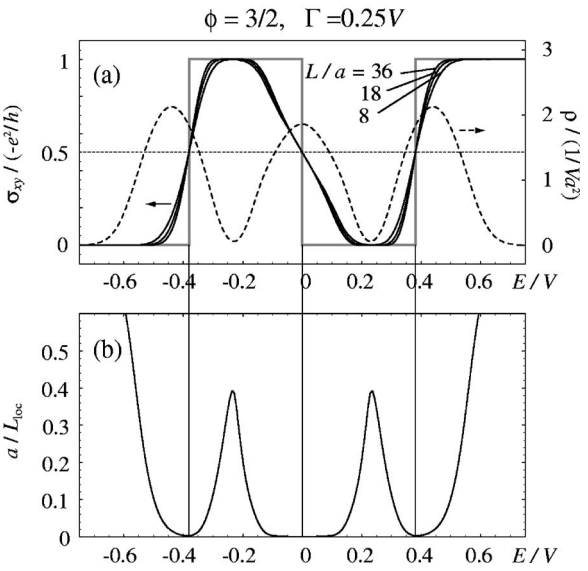

FIG. 2. (a) Hall conductivity σ_{xy} (solid line) and the density of states ρ (dashed) in the flux $\phi=3/2$ and the disorder $\Gamma/V=0.25$ with various sizes $L/a=8$, 18, and 36. The gray steplike line is an estimate of σ_{xy} as $L\to\infty$. (b) Inverse localization length estimated from the Thouless number. The vertical lines penetrating the panels represent the energies of the extended levels.

$$\delta E \approx 2\pi n_i v_0^2 \rho, \quad (10)$$

with ρ being the density of states per unit area. For a subband in the flux $\phi=p/q$, ρ is approximated as $1/(Wqa^2)$ with the subband width W, so that we obtain

$$\delta E \approx \frac{2\pi n_i v_0^2}{Wqa^2} \equiv \gamma. \quad (11)$$

The relation between Γ and γ is given by

$$\gamma = \frac{\pi}{2} \frac{\Gamma^2}{Wp}.$$

As a typical result, we show the calculation for the disordered system in the flux $\phi=3/2$ in Fig. 2. The top panel indicates the system size dependence of σ_{xy} and the density of states, and the bottom the inverse localization length $1/L_{\mathrm{loc}}$. The parameter of the disorder is set to $\Gamma/V=0.25$. In the clean limit, a Landau level splits into three separated subbands since $p=3$, and the Hall conductivity carried by each of the subbands is $\Delta\sigma_{xy}=1,-1,1$. Here and in the following we show σ_{xy} and $\Delta\sigma_{xy}$ in units of $-e^2/h$. When the system is disordered we find that the gaps between the subbands are smeared out while the Hall conductivity converges to quantized values around the density of states (DOS) dips, indicating the appearance of the Hall plateau. If we look at the size dependence of the Hall conductivity in the whole energy region, we see that σ_{xy} always approaches 1 in the area $\sigma_{xy}>1/2$ on increasing the size, and 0 in $\sigma_{xy}<1/2$, so we expect that in an infinite system the continuous function $\sigma_{xy}(E)$ changes into Hall plateaus connected by steps, as shown by the steplike line. Therefore we speculate that the points of $\sigma_{xy}=1/2$ are identified as the extended levels in an

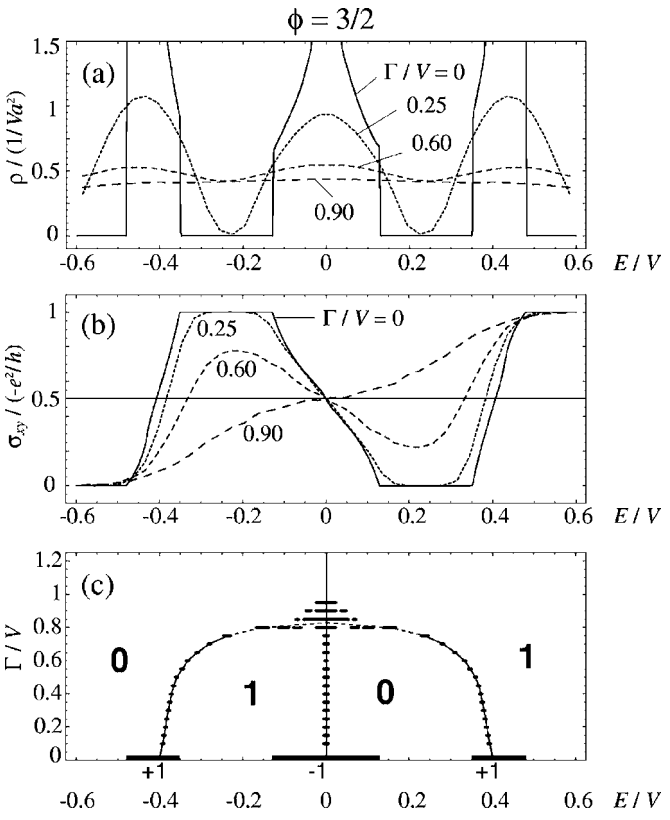

FIG. 3. (a) Density of states and (b) the Hall conductivity as a function of the Fermi energy at $\phi=3/2$ and $L=12a$ with several disorder parameters Γ/V. (c) Trace of the extended levels as a function of disorder, obtained by taking the energies of $\sigma_{xy}=n+1/2$ (in units of $-e^2/h$). The horizontal bars show the numerical errors. Integers in the enclosed areas represent the quantized Hall conductivities. The thick bars at $\Gamma=0$ and the integers below them indicate the ideal subbands and $\Delta\sigma_{xy}$, respectively.

infinite system, and they indeed agree with the energies where localization length diverges as shown in Fig. 2(b).

We can see similar tendencies in the size dependence of σ_{xy} in other fluxes as well, where the fixed points are always found at $\sigma_{xy}=n+1/2$ (n is an integer) in all the cases investigated. While each of the three subbands has one extended level at a certain energy in $\phi=3/2$, the localization generally depends on the Hall conductivity assigned to subbands. We have shown that a subband carrying zero Hall conductivity is completely localized in finite disorder strength.[12]

IV. EVOLUTION OF THE EXTENDED LEVELS

When we consider a situation where the disorder increases in the Hofstadter butterfly, we expect that the extended levels in the subbands move and merge on the energy axis in some way, and in large enough disorder, only one remains at the center of the Landau level. It would be nontrivial and intriguing to ask how they evolve as a function of disorder, and how different they are in various fluxes. Here we study the evolutions for some particular fluxes, on the assumption that the extended levels always exist at the energies of $\sigma_{xy}=n+1/2$ with integers n, and the region where $n-1/2<\sigma_{xy}<n+1/2$ in finite systems becomes $\sigma_{xy}=n$ in an infinite system.

We first show the results for the flux $\phi=3/2$ in Fig. 3. The top and middle panels indicate the density of states and the Hall conductivity, respectively, in a finite system $L=12a$ for several disorder parameters Γ. The bottom panel shows the traces of the extended levels obtained by just taking the energies of $\sigma_{xy}=n+1/2$. We observe that three extended levels get closer as the disorder increases, and contract into one at a certain Γ. The combination of three branches at a time is due to the electron-hole symmetry with respect to $E=0$, owing to the equal amounts of the positive and negative scatterers. If we break the symmetry by introducing imbalance between them, the evolution changes in such a way that two of them annihilate and one is left intact.[15]

The situation becomes a little complicated in a slightly larger flux $\phi=5/3$, as shown in Fig. 4. In the clean limit, we have five subbands carrying $\Delta\sigma_{xy}=-1,+2,-1,+2,-1$ from the bottom to the top. Since the second and the fourth bands pass through $n+1/2$ twice, each of them comes to have two extended levels in sufficiently small disorder on the present assumptions. On going to stronger disorder, one of the two extended levels experiences a pair annihilation with the lowest or highest subband, and only three extended levels are left as in $\phi=3/2$. When we start with a more complicated flux, we speculate that the Hall plateau structure is simplified one by one, going through analogs of the simpler fluxes nearby.

To check that there are actually two separated extended levels in a subband carrying $\Delta\sigma_{xy}=2$, we can make a scaling analysis in the Hall conductivity on varying the system size.

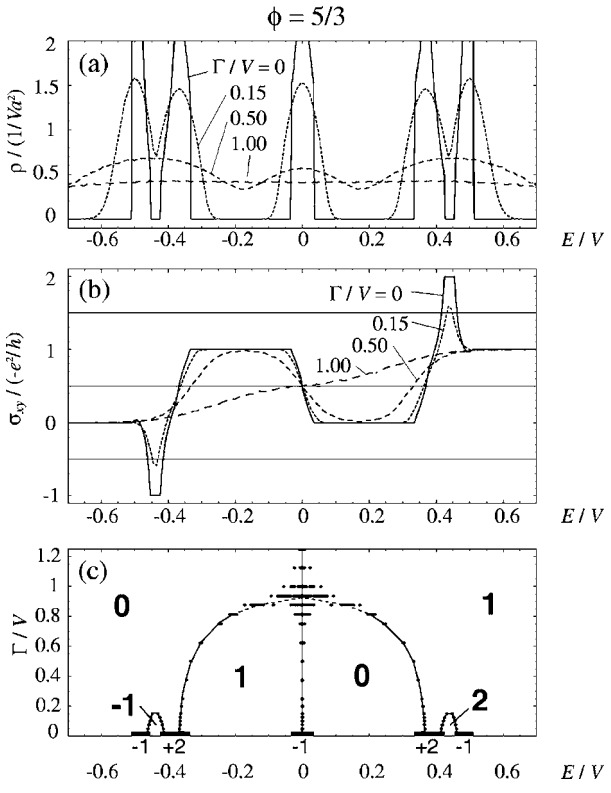

FIG. 4. Plots similar to Fig. 3 calculated for $\phi=5/3$.

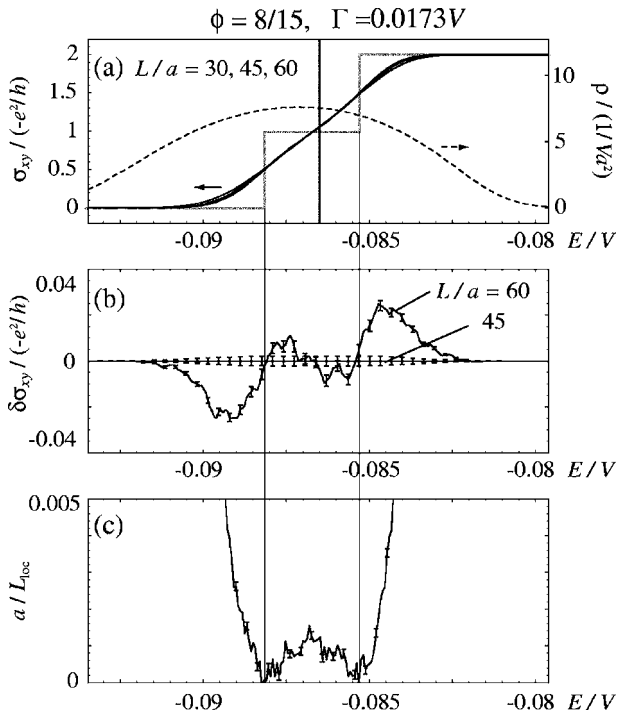

FIG. 5. (a) Hall conductivity σ_{xy} and the density of states ρ calculated for the lowest subband in $\phi=8/15$, carrying $\Delta\sigma_{xy}=-2e^2/h$, with the disorder $\Gamma/V=0.0173$ and various sizes $L/a=30$, 45, and 60. The gray steplike line is an estimate at $L\to\infty$. The vertical line at $E\approx-0.0865$ represents the energy region of the ideal subband. (b) Relative value of σ_{xy} in $L/a=60$ estimated from $L/a=45$. (c) Inverse localization length (in units of a) estimated from the Thouless number. Two vertical lines penetrating the panels represent the energies of the extended levels in an infinite system.

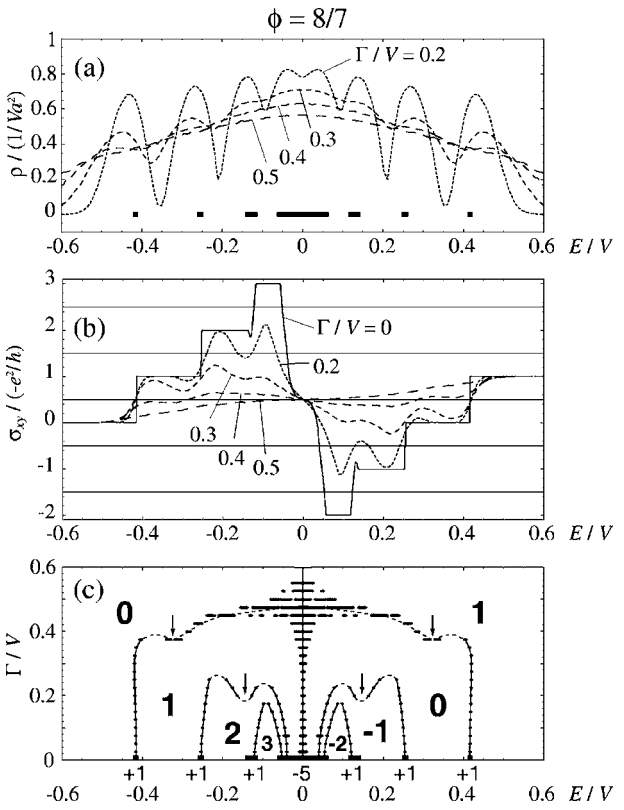

FIG. 6. Plots similar to Fig. 3 calculated for $\phi=8/7$. Arrows indicate the positions of the pair creations in the extended levels.

In the flux $\phi=5/3$, unfortunately, the large statistical error prevents us from resolving the splitting, but we can in a similar situation in another flux $\phi=8/15$, where the lowest subband carrying $\Delta\sigma_{xy}=2$. Figure 5 shows the Hall conductivity and the localization length for the lowest subband with disorder $\Gamma=0.0173V$. The difference in σ_{xy} between $L/a=45$ and 30, shown in the middle panel, indicates that σ_{xy} actually has turning points around $\sigma_{xy}=1/2$ and $3/2$. This is confirmed by the calculation of the localization length in the lowest panel, showing that $L_{\rm loc}$ diverges at those two energies, so it is quite likely that there are two extended levels in this subband in an infinite system.

A major difference from $\phi=5/3$ is that the ideal subband width is much narrower than the energy gap in the present case, so we can set the disorder in such a way that the states in the subband are completely mixed up but not with other subbands. We speculate that this situation makes the localization length smaller and enables us to resolve the separated extended levels in a finite-size calculation. We have another example where one subband has more than one extended level in an *anisotropic* modulated quantum Hall system. There $\sigma_{xy}(E)$ in a subband with $\Delta\sigma_{xy}=1$ has a nonmonotonic behavior crossing $\sigma_{xy}=1/2$ three times, so that three extended levels arise.[12]

Last we investigate a flux $\phi=8/7$, slightly away from $\phi=1$. Around this region the Landau level splits into a number of tiny subbands as seen in the original Hofstadter butterfly, just like the Landau levels in the usual 2DEG around zero field. This is actually understood as the Landau quantization in the magnetic Bloch band at $\phi=1$ caused by the residual flux $\phi-1$.[16] As seen in Fig. 6, each of these "Landau levels" equally carries the Hall conductivity of $\Delta\sigma_{xy}=1$ while the center one has a large negative value. It is highly nontrivial how the extended states evolves in increasing disorder in such a situation.

Figure 6 shows the disorder dependence of the density of states, the Hall conductivity σ_{xy}, and the traces of $\sigma_{xy}=n+1/2$ in a fixed system size $L=14a$ in $\phi=8/7$. Remarkably the result suggests that a pair creation of extended states can occur in increasing disorder, as indicated by the arrows in (c). In (b), we can see that this happens when a dip in $\sigma_{xy}(E)$ touches the line of $\sigma_{xy}=n+1/2$, where a pair of extended levels with opposite Hall conductivity are created as schematically shown in Fig. 7. In even stronger disorder, these newly created pairs annihilate with other extended levels in the lower and higher subbands.

To confirm the existence of a pair creation, we investigate the scaling behavior of the Hall conductivity $\sigma_{xy}(E)$ in a similar situation in $\phi=5/4$, for the smaller disorder $\Gamma=0.4V$ and the larger $0.525V$. The results in Fig. 8 show that the direction of the size dependence around the dip ($E/V\approx-0.2$) seems to change when passing through $\sigma_{xy}=0.5$, within the system size numerically available. This is consistent with the proposed scenario as in Fig. 7, while

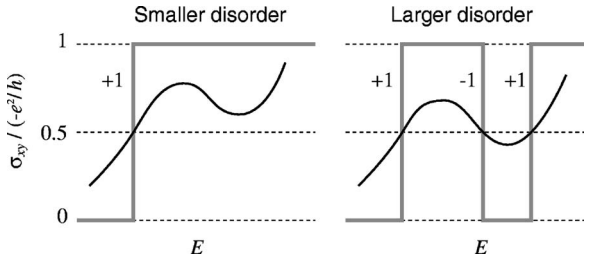

FIG. 7. Schematic figure of pair creation of the extended levels. The left and right panels show $\sigma_{xy}(E)$ in smaller and larger disorder, respectively, where a solid curve is for a finite system and a gray line for an infinite system. The pair of extended levels are newly created when a dip touches the line of $\sigma_{xy}=0.5(-e^2/h)$.

we need further extensive work to confirm that the tendency remains toward the infinite system.

For the usual 2DEG without a periodic potential, there has been a long debate about the fate of the extended states in the Landau levels in the strong disorder limit in a weak magnetic field. It has been argued that all the extended states float up in the energy axis with increasing disorder and the system finally becomes an insulator.[17–19] Numerical calculations in tight-binding lattice models, on the other hand, showed that the states with negative Hall conductivity move down from the tight-binding band center, to annihilate with the extended states in the lower Landau levels.[20–22] Our theory may suggest a somewhat different story where pair creations of the extended states occur, since we actually observe similar dips in $\sigma_{xy}(E)$ around higher Landau levels in a disordered nonperiodic 2DEG.

We also remark that the evolution of the extended levels generally depends on the correlation lengths of the disorder potential. It was shown in the tight-binding model that the pair annihilation of the extended states with positive and negative Hall conductivity do not occur in the long-range disorder.[23,24] In our problem, the scenario of the pair creation might change in correlating disorder, since the appearance of the dips in $\sigma_{xy}(E)$ is due to the inter-Landau-level mixing,[25,26] and thus is suppressed by long-range scatterers. This should be addressed in future work.

V. HALL PLATEAU DIAGRAM

We extend the analysis to general fluxes to look into the quantum Hall effect over the whole region of the Hofstadter butterfly. Figure 9 shows (a) the Hall conductivity, (b) the density of states, and (c) the localization length in disordered systems with $\Gamma/V=0.25$, plotted against the Fermi energy and the magnetic field. The solid lines in Fig. 9(a) represent the extended levels in an infinite system, and the enclosed areas are the Hall plateaus with the quantized value of σ_{xy}, where we again assume that the extended levels in an infinite system coincide with the energies of $\sigma_{xy}=n+1/2$ in a finite system. In the density of states [Fig. 9(b)], we recognize valleys in the contour plot as the remnants of the minigaps, and some of them can be associated with the Hall plateaus in (a). For instance, a pair of valleys between $\phi=1$ and 2 inside the Landau level corresponds to two major plateaus with $\sigma_{xy}=0$ in $0<E<0.5V$ and $\sigma_{xy}=1$ in $-0.5V<E<0$.

In Fig. 9(c), we see that the energy region with large localization length becomes broad particularly around integer fluxes. There the cluster of subbands widely spreads along the energy axis, and thus the states are less easily mixed. We also find that the upper and lower branches of the spectrum in $\phi\gtrsim 2$, carrying zero net Hall conductivity, are all localized, as seen in the particular case $\phi=3$.[12] The localization length is smaller for larger ϕ in those branches, mainly because the mixing of the states becomes stronger in narrower subbands.

In Fig. 10, we show the Hall plateau diagrams and the density of states for the different disorder parameters $\Gamma/V=0.15$ and 0.5, which exhibit the dependence on Γ together with Figs. 9(a) and 9(b). We can see that the small Hall plateaus coming from the fine gap structure gradually disappear as the disorder becomes larger, and the only extended level is left at the center of the Landau level in the strong disorder limit. We here notice in $\Gamma/V=1.5$ that the two largest plateaus between $\phi=1$ and 2 mentioned above are more easily destroyed around $\phi=1$ than around $\phi=2$, or the right end is detached from $\phi=1$ while the left sticks to $\phi=2$. This is because the tiny gaps around $\phi=1$ are easily swallowed up by the large density of states around the center.

VI. SELF-SIMILARITY

The interesting observation in the Hofstadter butterfly is that the identical spectrum with *the identical distribution of the Hall conductivity* repeatedly appears in different fluxes. In Fig. 1(b), we can see that the spectrum and the Hall conductivity at ϕ correspond to the middle part of $\phi+2$ with the

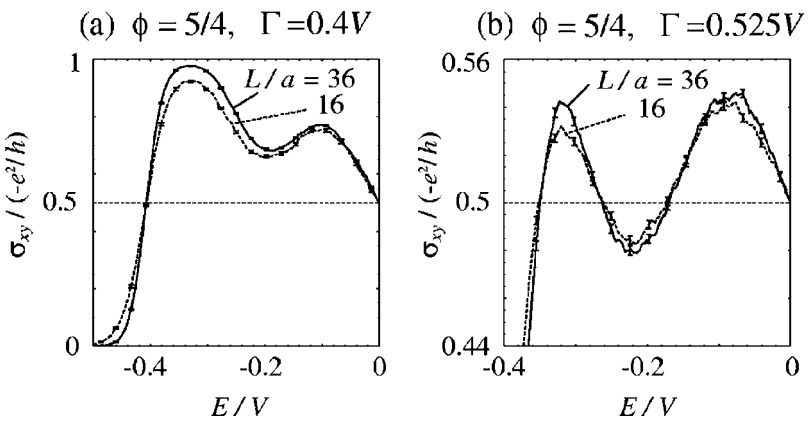

FIG. 8. Hall conductivity σ_{xy} in the flux $\phi=5/4$ and the disorder $\Gamma/V=$ (a) 0.4 and (b) 0.525 (in different vertical scales), with the system sizes $L/a=16$ and 36.

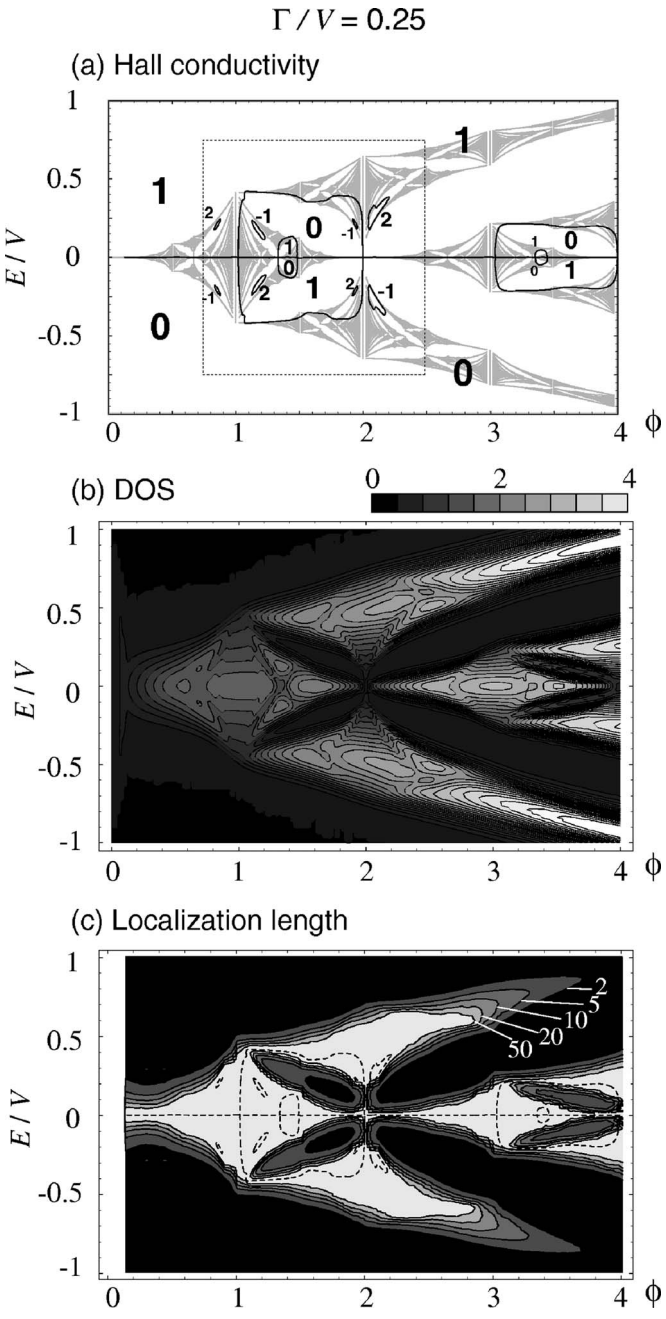

FIG. 9. (a) Hall plateau diagram in the lowest Landau level at the disorder $\Gamma/V=0.25$, plotted against the magnetic flux and the Fermi energy. Solid lines show the energy of $\sigma_{xy}=n+1/2$ (n is an integer), which are identified as the extended levels in an infinite system, and the integers indicate the Hall conductivity in units of $-e^2/h$. The ideal spectrum is shown as the gray scale. (b) Corresponding plots for the density of states in units of $1/(Va^2)$. (c) Localization length in units of a. The dashed lines indicate the extended levels shown in (a).

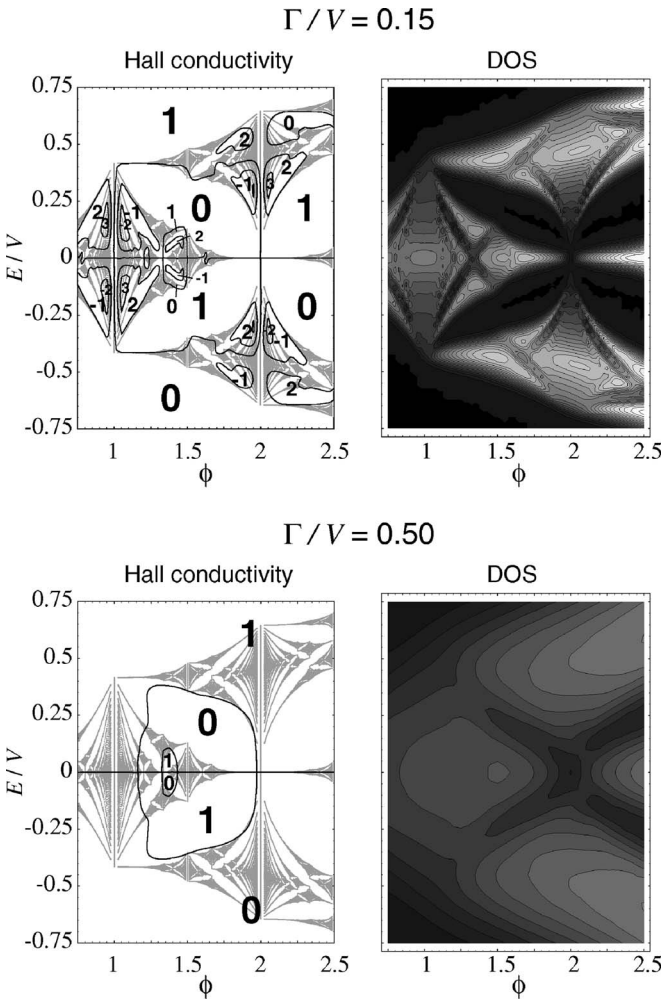

FIG. 10. Hall plateau diagram (left) and the density of states (right) in the disorder $\Gamma/V=0.15$ (top) and 0.5 (bottom), plotted against the magnetic flux and the Fermi energy. The corresponding parameter region is shown as the dashed line in Fig. 9(a).

top and bottom branches excluded, so that the entire structure repeats over $\phi+2m$ with integer m. The proof of the correspondence is presented in the Appendix. We note that, while the Hofstadter butterfly has similar gap structures everywhere in a fractal fashion, the Hall conductivities in the corresponding gaps do not always coincide. An example of the incomplete correspondence is seen between ϕ and $\phi'=1/(1-1/\phi)$ (such as $\phi=3$ and $3/2$). In the tight-binding model, it was shown that the distributions of the Hall conductivity within a cluster resemble each other up to a scale factor among some series of fluxes.[27]

In the following we show that, in the presence of disorder, the corresponding clusters with identical Hall conductivity have qualitative agreement also in the localization length. Here we particularly take a pair of fluxes $\phi=3/2$ and $7/2$, in both of which the central three subbands have the Hall conductivity $(1,-1,1)$. In Fig. 11 we compare the disorder effects on the density of states and the localization length. We set the disorder as $\Gamma=0.25$ and 0.20 for $\phi=3/2$ and $7/2$, respectively, so that the renormalized DOS broadening $\gamma/W_{\rm tot}$ is equivalent, where we defined γ by putting in Eq. (11) the full width of three subbands $W_{\rm tot}$. The result shows that the densities of states are broadened equivalently as expected, and that the localization lengths $L_{\rm loc}$ then agree qualitatively without any scale factors.

Figure 11(c) shows the evolution of the extended levels as a function of the disorder, which are obtained by taking the

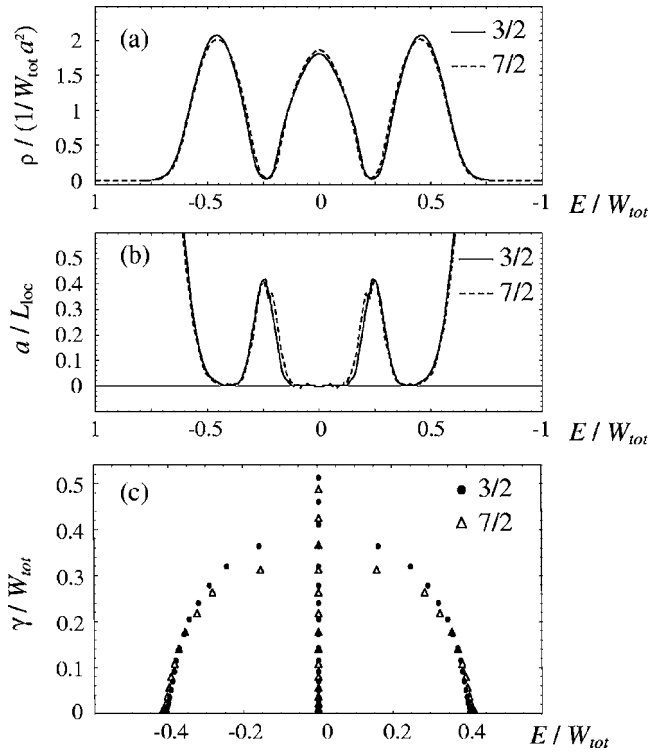

FIG. 11. (a) Density of states and (b) the inverse localization length calculated for disordered systems with $\phi=3/2$ (solid lines) and 7/2 (dashed). The energy scale is normalized by the whole width of the Landau level in the ideal system, W_{tot}, and the density of states in units of $1/(W_{\mathrm{tot}}a^2)$. The parameter of the disorder is $\gamma/W_{\mathrm{tot}}=0.035$. (c) Evolutions of the extended levels with changing disorder γ, in $\phi=3/2$ (filled circles) and 7/2 (triangles).

points of $\sigma_{xy}=1/2$. Three extended levels in $\phi=3/2$ and $7/2$ evolve in a parallel fashion with the disorder strength γ/W_{tot}, where they come closer as γ becomes larger and combine into one at $\gamma/W_{\mathrm{tot}}\approx 0.4$. The critical disorder at which the combination occurs is slightly smaller in $\phi=7/2$ than in $3/2$, presumably because in $\phi=7/2$ the level repulsion from the outer subbands (out of the figure) pushes the states in the central three subbands toward the center of the spectrum and that enhances the contraction of the extended levels. We expect that the critical behavior of the three extended levels at the combing point is universal, but we could not estimate the critical exponent in this simulation due to statistical errors. The evolution of the plateau diagram should become basically similar among $\phi+2m$, so we know all from the information of the first unit.

The similar subband structures with the identical Hall conductivity can be found in other hierarchies in the Hofstadter butterfly. The smallest unit that we have found is schematically shown in Fig. 12, where the structure indicated by A between $\phi=0$ and 1 repeats over the entire region. We can show similarly that each unit has the identical distribution of the number of states to each subband so that we have the identical Hall conductivity for every gap. We expect that the localization length in each single unit A becomes similar when the disorder is weak enough that the mixing among different units can be neglected.

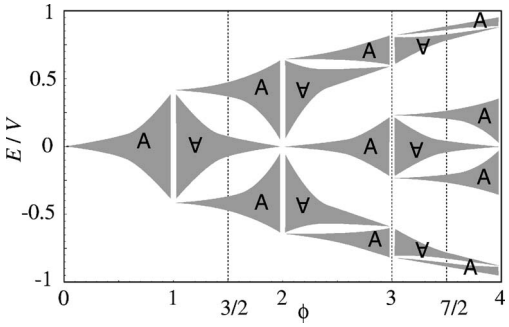

FIG. 12. Schematic diagram showing decomposition of the Hofstadter butterfly into identical units, where the gap structure and the Hall conductivity inside each gap coincide. The letter A indicates the direction.

VII. CONCLUSION

We studied the quantum Hall effect in a Landau level in the presence of a two-dimensional periodic potential with short-range disorder potentials. It is found that, in all the cases we studied, the Hall conductivity becomes size independent at $\sigma_{xy}=n+1/2$ (in units of $-e^2/h$), and those points are identified as the extended levels in an infinite system. We propose a possible model for the evolution of the extended levels by tracing $\sigma_{xy}=n+1/2$, which predicts that a subband with $\sigma_{xy}=n$ has n (or more) bunches of extended levels, and possibly that pair creation in the extended level can occur in increasing disorder, as well as pair annihilation. We also find that the clusters of subbands with an identical Hall conductivity, which compose the Hofstadter butterfly in a fractal fashion, have a similar localization length in the presence of the disorder.

ACKNOWLEDGMENTS

This work has been supported in part by the 21st Century COE Program at Tokyo Tech "Nanometer-Scale Quantum Physics" and by a Grant-in-Aid for COE (Grant No. 12CE2004 "Control of Electrons by Quantum Dot Structures and Its Application to Advanced Electronics") from the Ministry of Education, Science and Culture, Japan. One of the authors (M.K.) is supported by a Grant-in-Aid for Scientific Research from the Ministry of Education, Science and Culture, Japan. Numerical calculations were performed in part using the facilities of the Supercomputer Center, Institute for Solid State Physics, University of Tokyo.

APPENDIX: CONCIDENCE IN THE HALL CONDUCTIVITY

The equivalence in the gap structure with the Hall conductivity between ϕ and $\phi+2$, discussed in Sec. VI, is explained as follows. The number of subbands in a Landau level is given by the numerator of the magnetic flux ϕ, so that we have p bands in $\phi=p/q$ and $p+2q$ bands in $\phi+2$. Each single subband in ϕ and $\phi+2$ consists of the equal number of states per unit area, $1/(qa^2)$, since two fluxes have a common denominator q so that they have equal foldings of the Brillouin zone. We can then see that each of the top and

bottom branches in $\phi+2$ contains q subbands, because each has a constant number of states $1/a^2$ as explained in Sec. II. Thus the number of subbands in the middle part in $\phi+2$ (the top and bottom branches removed) becomes $(p+2q)-2\times q=p$, which is equal to the total subbands in ϕ. Now we see that the corresponding spectra between ϕ and $\phi+2$ have the same number of subbands with equal numbers of states, so we come to the conclusion that the Hall conductivity becomes identical between the corresponding gaps, by using the Středa formula (9).

[1] D. R. Hofstadter, Phys. Rev. B **14**, 2239 (1976).
[2] D. J. Thouless, M. Kohmoto, M. P. Nightingale, and M. den Nijs, Phys. Rev. Lett. **49**, 405 (1982).
[3] C. Albrecht, J. H. Smet, K. von Klitzing, D. Weiss, V. Umansky, and H. Schweizer, Phys. Rev. Lett. **86**, 147 (2001); Physica E (Amsterdam) **20**, 143 (2003).
[4] M. C. Geisler, J. H. Smet, V. Umansky, K. von Klitzing, B. Naundorf, R. Ketzmerick, and H. Schweizer, Phys. Rev. Lett. **92**, 256801 (2004).
[5] D. Pfannkuche and R. R. Gerhardts, Phys. Rev. B **46**, 12606 (1992).
[6] U. Wulf and A. H. MacDonald, Phys. Rev. B **47**, 6566 (1993).
[7] Y. Tan, J. Phys.: Condens. Matter **6**, 7941 (1994); Phys. Rev. B **49**, 1827 (1994).
[8] Y. Hatsugai, K. Ishibashi, and Y. Morita, Phys. Rev. Lett. **83**, 2246 (1999).
[9] K. Yang and R. N. Bhatt, Phys. Rev. B **59**, 8144 (1999).
[10] B. Huckestein, Phys. Rev. Lett. **72**, 1080 (1994).
[11] B. Huckestein, Rev. Mod. Phys. **67**, 357 (1995).
[12] M. Koshino and T. Ando, J. Phys. Soc. Jpn. **73**, 3243 (2004).
[13] P. Středa, J. Phys. C **15**, L718 (1982).
[14] T. Ando and Y. Uemura, J. Phys. Soc. Jpn. **36**, 959 (1974).
[15] M. Koshino and T. Ando, Physica E (Amsterdam) **29**, 588 (2005).
[16] M. C. Chang and Q. Niu, Phys. Rev. Lett. **75**, 1348 (1995).
[17] H. Levine, S. B. Libby, and A. M. M. Pruisken, Phys. Rev. Lett. **51**, 1915 (1983).
[18] D. E. Khmelnitskii, Phys. Lett. **106A**, 182 (1984).
[19] R. B. Laughlin, Phys. Rev. Lett. **52**, 2304 (1984).
[20] T. Ando, Phys. Rev. B **40**, 5325 (1989).
[21] D. Z. Liu, X. C. Xie, and Q. Niu, Phys. Rev. Lett. **76**, 975 (1996).
[22] D. N. Sheng and Z. Y. Weng, Phys. Rev. Lett. **78**, 318 (1997).
[23] T. Koschny, H. Potempa, and L. Schweitzer, Phys. Rev. Lett. **86**, 3863 (2001).
[24] D. N. Sheng, Z. Y. Weng, and X. G. Wen, Phys. Rev. B **64**, 165317 (2001).
[25] T. Ando, Y. Matsumoto, and Y. Uemura, J. Phys. Soc. Jpn. **39**, 279 (1975).
[26] T. Ando, J. Phys. Soc. Jpn. **55**, 3199 (1986).
[27] H. Ritter, Z. Phys. B: Condens. Matter **56**, 185 (1984).